

Analysis of Interpolation based Image In-painting Approaches

Mustafa ZOR¹ Erkan BOSTANCI² , Mehmet Serdar GÜZEL^{3*} , Erinç KARATAŞ⁴

^{1,2,3,4} Ankara University, Ankara,TR

Corresponding author email*: mguzel@ankara.edu.tr

Interpolation and internal painting are one of the basic approaches in image internal painting, which is used to eliminate undesirable parts that occur in digital images or to enhance faulty parts. This study was designed to compare the interpolation algorithms used in image in-painting in the literature. Errors and noise generated on the colour and grayscale formats of some of the commonly used standard images in the literature were corrected by using Cubic, Kriging, Radial based function and High dimensional model representation approaches and the results were compared using standard image comparison criteria, namely, PSNR (peak signal-to-noise ratio), SSIM (Structural SIMilarity), Mean Square Error (MSE). According to the results obtained from the study, the absolute superiority of the methods against each other was not observed. However, Kriging and RBF interpolation give better results both for numerical data and visual evaluation for image in-painting problems with large area losses.

Keywords: Image in-painting, Interpolation, Cubic interpolation, Kriging interpolation, Radial based function, High dimensional model representation

1. Introduction

When analogue cameras were widely used, the photographs we kept in print were at risk of aging, fading, wear, and thus loss of information. With the advent of digital cameras, the development of computer and storage, and even cloud storage, our habit of storing photographs in print has evolved accordingly. However, this did not eliminate the risk of information loss of our photos. Errors or loss of information were observed in digital photographs during the acquisition and transmission of the photograph. Some of these may be related to the direct quality of the photograph, such as blur and noise, and in some cases, loss of information in certain areas of the picture. In addition, there may be errors such as the unintentional incorporation of undesirable objects into the photo frame during the photo shoot.

Some methods have been developed due to requirements such as eliminating the lack of information in photographs or eliminating unwanted areas. Bertalmio et al. (2000) developed in-painting terminology. In-painting is the art of modifying a picture or video in a way that cannot be easily detected by an ordinary observer and has become a major research area in image processing (Bugeau et al. 2010). The missing or undesirable portion of the image is completed by using intensity levels on adjacent pixels. However, the image in-painting will not be able to restore the original form of the missing part in the picture, it will only fill the missing or undesirable parts, close to the original (Amasidha et al. 2016).

The methods developed for in-painting can be grouped under three main headings.

- **Texture synthesis:** The basis of this approach is the self-similarity principle. It is based on the assumption that similar structures in a picture are often repeated (Bugeau et al. 2010).
- **Exemplar-based approach:** The missing region is filled with information from the known region at the patch level.
- **Partial differential equations and variation-based diffusion techniques:** The method of partial differential equations fills the regions to be uniformly propagated along the isophot directions from neighboring regions along the direction of isophot. The method, which gives good results for small areas, causes turbidity in larger areas. Variation methods address the problem in the form of finding the extremes of energy

functions. However, these models only aim at dealing with non-textural in-painting. The difficulty of real in-painting problems is due to the rapid changes of the isophot and the roughness of the image functions (Chang and Chongxiu 2011).

In addition to this, methods have been developed that consider interiors as an interpolation problem and apply different interpolation techniques to complete the missing areas in the images (Guzel, 2015 and Mutlu et. al., 2014).

In this study, we aimed to evaluate the interpolation methods to handle the image in-painting process as an interpolation problem as the main contribution. State-of-the-art methods were tested on a generated dataset which was subject to both noise and corruption. These methods were then assessed based on their SSIM, PNSR and MSE in a quantitative evaluation. A qualitative evaluation was also performed on the results to ensure that the interpolation approach yielded visually appealing images (Bostanci, 2014 and Seref et. al, 2021).

The rest of the paper is structured as follows: Section 2 presents the current literature and background on the interpolation approaches employed in the paper. This section is followed by Section 3 where the dataset and the evaluation approach is elaborated. Section 4 presents both quantitative and qualitative results, finally the paper is concluded in Section 5.

2. Literature Review and Background

2.1 Cubic Interpolation

This interpolation is one of the common methods used to estimate unknown points. It generates results with smoother transitions and lower error rate than other interpolation techniques with polynomials. It is a commonly used method for filling lost pixels. When an interpolation of surface values is desired in a two-dimensional field, it can be formulated as follows.

On a unit square, if the surface values at the corners and the partial derivative values at these points are known, the convergence values of the points within the square can be obtained by polynomial (1)

$$p(x, y) = \sum_{i=0}^3 \sum_{j=0}^3 a_{ij} x^i y^j \quad (1)$$

The known corner values of the surface and the partial derivative values (f_x, f_y, f_{xy}) in the x and y direction which can be obtained from the corner points. The polynomial is obtained by replacing the required equations with unknown coefficients for a_{ij} which can be solved using matrix format to express the polynomial exactly.

2.2 Kriging Interpolation

Kriging is a geostatistics interpolation method that takes into account the distance and degree of variation between known points when estimating values at unknown points (Firas and Jassim 2013). This approach uses the values of the entire sample to calculate an unknown value. Kriging assumes that the distance or direction between sample points reflects a spatial correlation that can be used to explain variation on the surface. In kriging interpolation, a mathematical function is applied to all points of a specified number or a specified radius to determine the estimation value of each unknown point. The closer the point is, the higher value the weights have. Kriging is the most appropriate approach when there is a spatially related distance or directional trend in the data (spatial auto-correlation) and calculated as follows:

$$\hat{P}^* = \sum_{i=1}^N \lambda_i P_i \quad (2)$$

where $N:k \times k$ (sample) is the total number of intact pixels, \hat{P}^* : pixel to be interpolated, $P_i : k \times k$ intact pixels in the block, $\lambda_i : k \times k$ weights of the intact pixels in the block ($\sum_{i=1}^N \lambda_i = 1$)

. Kriging interpolation, chooses values of λ_i in order to minimize the interpolation variance ($\sigma^2 = E\left[\left(P - \hat{P}^*\right)^2\right]$).

Two steps are required for Kriging interpolation:

1. Dependency rules: Constructing variograms and covariance functions to predict statistical dependence (spatial autocorrelation) based on the autocorrelation model (fitting a model).

The Variogram is a function of distance and direction that separates the two positions used to measure dependence. Variogram is defined as the variance of the difference between two variables at two different points and is calculated as:

$$2\gamma(h) = \frac{1}{n} \sum_{i=1}^N [P(x_i) - P(x_i + h)]^2; \quad P(x_i), P(x_i + h): x_i, x_i + h \quad (3)$$

2. Estimation: Estimating unknown values.

The data is used twice to perform these two steps.

Jassim (2013) creates damaged images by using 4 different masks on 10 different grayscale images and uses Kriging interpolation to remove them. Sapkal and Kadbe (2016) also do in-painting using Kriging interpolation. In this study, the results are obtained by using the same masks on 5 different grayscale images.

Sapkal et al. (2016) used Kriging interpolation to remove several types of masks. In the study, the same dataset was used with a different set of masks.

Awati et al. (2017) conducted a study on troubleshooting colour images using modified Kriging interpolation. They separate colour images into RGB components and apply separate interpolation to each component. In practice, 3x3 matrices are used. The masks they use consist of vertical, horizontal and curved lines. They make separate trials for 1,2,3 and 4 pixel thicknesses as line thicknesses in each mask and evaluate the results.

2.3 Radial Basis Functions

Chang and Chongxiu (2011) define a mapping between the coordinates and colours of the image pixels, and implement an algorithm based on radial-based functions to generate the best approximation of this mapping in a given neighborhood. Radial-based functions are means of approximating a multivariable function as a linear combination of univariate functions. It is one of the methods that provides good results for the interpolation of scattered data. In order to increase the accuracy of their solutions and reduce the complexity of the algorithm, researchers create the pixel-by-pixel zoom function. For larger loss areas, interpolation of different overlapping coefficients is used.

Wang and Qin (2006) propose an algorithm for image in-painting based on compactly supported radial basis functions (CSRBF). The algorithm transforms the 2-D image in-painting problem from a 3-D point set into a surface reconstruction problem. First, a covered surface is constructed for approximation to the set of dots obtained from the damaged image using radial based functions. The values of the lost pixels are then calculated using this surface.

2.4 High Dimensional Model Representation and Lagrange Interpolation

Karaca and Tunga (2016), who consider image in-painting as an interpolation problem, have designed this problem by using the HDMR method and Lagrange interpolation, which allows a multivariate function to be expressed as the sum of multiple functions with less variables.

Normally grayscale images are represented as functions with two variables $f(x, y)$, x : number of rows, y : number of columns. Similarly, coloured images are represented by a function of three variables $f(x, y, z)$. In order to apply HDMR, the copy of the image itself is added as an

additional dimension. In other words, a grayscale image, $f(x, y, n)$, $n = 1, 2$; and the colour image is expressed as $f(x, y, z, n)$, $z = 1, 2, 3$, $n = 1, 2$ (RGB channels).

HDMR expansion for a multivariate function; fixed term is defined as the sum of functions of one variable, functions of two variables and others.

$$f(x_1, x_2, \dots, x_N) = f_0 + \sum_{i_1=1}^N f_{i_1}(x_{i_1}) + \sum_{i_1, i_2=1}^N f_{i_1 i_2}(x_{i_1}, x_{i_2}) + \dots + f_{12 \dots N}(x_1, x_2, \dots, x_N) \quad (4)$$

In general, functions are represented up to univariate or bivariate functions, and the remainder is ignored as an approximation error. The function created for grayscale images can be fully represented when it is extended up to two-variable functions in the HDMR expansion (Altın and Tunga 2014). The researchers presented a representation by making up to three variable functions for in-painting with colour images and aimed to estimate the lost pixels by applying them with Lagrange interpolation.

In another study, Karaca and Tunga (2016) also studied the in-painting of a rectangular area using the same method. They tried 5x5, 10x10 and 20x20 pixel dimensions on different images for the in-painting area.

The algorithms used for in-painting in the literature have also been used for noise removal. Jassim (2013) tried the Kriging algorithm for salt & pepper noise reduction. For noise of varying intensity, it first *detects* noise using an 8x8 pixel filter on the image, and then applies Kriging interpolation to correct incorrect pixel values in this area.

3. Material and Method

3.1 Material

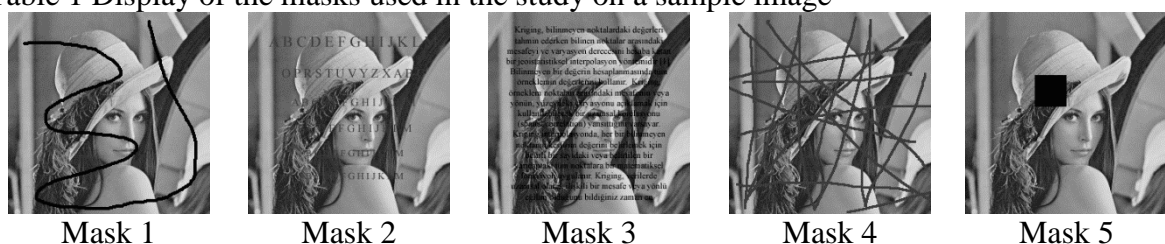
The internally stained images obtained from the methods used in the studies and their originals were presented with PSNR and SSIM criteria. In addition, although the masks used in the studies seem similar to each other, they have differences. This is a limitation for the exact comparison of algorithms. In order to make a full comparison of the algorithms proposed in this part of the study, we compared the results obtained by using the same masks and images and each of the methods.

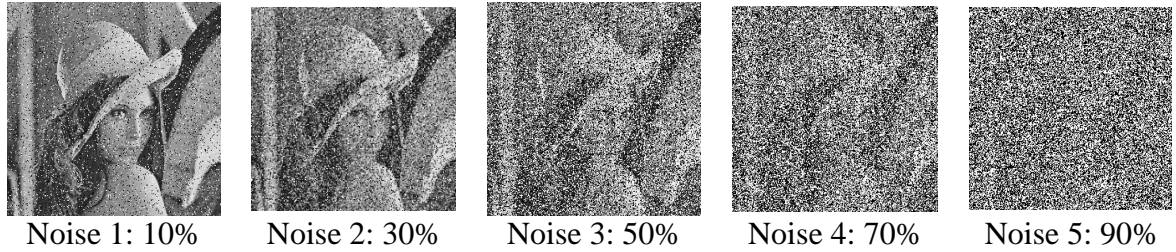
256x256 grayscale and colour images were used to compare the algorithms. The images used were selected from the images commonly used in image processing research: Lena, Mandril, Peppers, Jetplane and House. The masks applied to the images are created as follows:

- Mask 1: simple curve, drawn with 4 pixel-thick pencil
- Mask 2: A non-condensed font consisting of several lines between 12-19 fonts,
- Mask 3: Intense font created with 12 font letters,
- Mask 4: Intense scratches of oblique, horizontal and vertical lines drawn with a 4-pixel-thick pencil,
- Mask 5: Frame created with a size of 40x40 pixels.

In addition, to test the noise reduction efficiency of interpolation methods, masks created with salt & pepper noise were applied. Their density levels are Noise 1: 10%, Noise 2: 30%, Noise 3: 50%, Noise 4: 70% and Noise 5: 90%, respectively. For instance, the presentation of the grayscale Lena image with the masks to be used is demonstrated in Table 1.

Table 1 Display of the masks used in the study on a sample image





In all of the algorithms, corrected images were obtained by calculating only unknown pixel values and the obtained images were compared with the original image using PSNR (peak signal-to-noise ratio) and SSIM (Structural SIMilarity) criteria. In order to determine the unknown pixel values, the difference between the pixel values between the original image and the false image was taken and the non-0 pixel values were tried to be estimated by the algorithms. In the comparison of the results with the actual image, the mean square error (MSE), which is a part of the SSIM and PSNR criteria, is indicated.

3.2 Method

The evaluation presented in this study employs a number of various interpolation techniques, namely, Two-dimensional cubic interpolation, Kriging interpolation, Interpolation with radial based functions (RBF), Interpolation using High Dimensional Model Representation. These techniques are detailed in the following.

3.2.1 Two-dimensional cubic interpolation

For this method, x , y : row, column coordinate values of known pixels, v : pixel values, x_q , y_q : coordinate values of the desired pixels, cubic: to be used as input parameters for the interpolation. After the information of the two-dimensional image is put into the form that the function can use, the function is executed and the new pixel values are updated.

3.2.2 Kriging interpolation

For this method, kriging (x_i , y_i , z_i , x , y) and auxiliary functions presented by Schwanghart and Kuhn (2010) were used (x_i , y_i : row, column coordinate values of known pixels, z_i : pixel values, x , y : to be the value of the coordinate values of the desired pixels). 256x256 pixel images were used along with masks of size 16x16 pixels masks and noise densities defined in 8x8 pixels neighbourhood. The unknown values in each sub-image were calculated using Kriging function.

In this way, it is ensured that the unknown points in the sub-images are related to all pixel values in the sub-images. The 8x8 pixel size has enough data for noise reduction. However, the Kriging algorithm did not work for Noise5 with a 90% density (see Table 1). Therefore, only 16x16 pixels are used for Noise5. On the other hand, although the calculation method by sub-images is suitable for scattered errors, it will not be suitable for an internal painting problem as in Mask5. Therefore, for the case in Mask5, the image in-painting is reduced to a 90x90 pixel image size that will take the center of the lost frame area (40x40 pixels) and the function is run on this 90x90 pixel neighbourhood.

3.2.3 Interpolation with radial based functions (RBF)

The approach of (Foster 2009) was adopted in order to compute the RBF function in a similar fashion with the Kriging interpolation where subimages are used for the computation.

3.2.4 Interpolation using High Dimensional Model Representation

For this method, following the approach of Tunga and Koçanoğulları (2017) study; constant, one-variable and two-variable functions representing grayscale images; The fixed, one, two and three variable functions representing the coloured images were found and the missing areas on these functions were corrected by interpolation approach. In this section, spline for interpolation of one-dimensional functions and cubic interpolation for interpolation of two-dimensional functions were implemented.

These methods can be applied directly to grayscale images which can be expressed as two variable functions. Interpolation of coloured images were obtained by applying the above interpolations separately to the three layers of the images. At this point, there is no difference between the method applied to grayscale images. For the calculations, the same algorithms were applied to the red, green, blue (RGB) layers three times and then combined to produce corrected colour images.

4. Results

In-painting results were obtained using the various interpolation methods discussed above. All the results obtained for a sample are presented in Figures 1 (in grayscale) and 2 (in colour).

The numerical comparison results obtained from all images are summarized in Table 2 for grayscale and in Table 3 for colour images. The results of two-dimensional cubic interpolation, Kriging interpolation, RBF interpolation and YBMG interpolation are shown in four large blocks. Orange, blue, green intracellular staining was used to compare the outputs of the four methods. For example, in the PSNR values of 4 different methods used to remove Mask 1 in the colour Lena image, 2-dimensional cubic interpolation has the highest value. This cell was stained with orange. The highest SSIM values of the four methods were painted with blue, while the lowest MSE values of the four methods were painted with green. By means of this staining, it is better to observe which method gives better results in which situation.

In addition, the data of four different methods were compared with the one-way ANOVA test to determine whether there was a difference between the methods in terms of PSNR, MSE and SSIM. There was no difference between the methods in terms of PSNR, MSE and SSIM values in the evaluation ($p = 0.997$, $p = 0.998$, $p = 0.986$ for gray images, $p = 0.974$, $p = 0.994$, $p = 0.988$ for color images, respectively).

In addition, in order to compare the numerical results of the four methods, the difference between the maximum value and the smallest value of the PSNR and SSIM results obtained for each image and mask was attempted to be observed as a percentage change. These ratios are presented as Figures 3 and 4.

PSNR and MSE values are directly related to each other. As it is known, the MSE value is part of the PSNR criterion. The PSNR value is inversely proportional to the logarithm of the square root of MSE (5) Therefore, it is essential to have the lowest MSE when PSNR is highest.

$$PSNR = 20 \log_{10} (255 / \sqrt{MSE}) \quad (5)$$

In addition, the formula of MSE (6) is built on differences in density levels between the two images.

$$MSE = \frac{1}{NM} \sum_{x=1}^N \sum_{y=1}^M [f(x, y) - g(x, y)]^2 \quad (6)$$

In other words, the closer the pixel values in the same position in the two images are, the closer the MSE value is to 0. We understand that the smaller the MSE value and the higher the PSNR, the better the results. On the other hand, the SSIM criterion was formulated to measure luminance, contrast and structural correlation between the two images. The results obtained from functions comparing these three criteria separately are multiplied to find the SSIM value. Each function takes values in the range 0-1, as a result SSIM has values from 0 to 1. The SSIM value approaches to unity when the correlations are high, *i.e.* the images are similar. Although the PSNR and SSIM calculations do not seem to be alike, there are studies showing that these are analytically related (Horé and Ziou 2010). Therefore, SSIM and PSNR values are expected to be higher in a well obtained in-painting.

As a result of this evaluation; In Table 2 and Table 3, it will be natural for the cells stained with orange, blue and green to coexist. However, in some cases it is observed that this association is not preserved, but this is due to very small differences that can be ignored. Therefore, the outputs we obtained do not contradict theoretical knowledge.

For each image and method in Figure 3 and Figure 4, it was tried to observe the percentage change between the methods by the ratio of the highest and lowest obtained score differences to the lowest value. As can be observed here, the numerical comparison results for images obtained by in-painting are generally very close to each other. The difference in SSIM values does not exceed 5%. PSNR values are mostly within the 5% change band.

In addition, according to the statistics obtained from the one-way ANOVA test, it was confirmed that there was no difference between the methods in numerical evaluation scales. Therefore, it is observed that the methods do not have absolute superiority to each other in terms of in-painting results.

If the methods of application are taken into consideration, the in-painting problem in Mask 5 will need to be evaluated separately. In other masks, the problem of internal painting is scattered throughout the image, where it focuses on a specific area. Therefore, in Kriging and RBF interpolation methods, we focused on the 90x90 pixel area in order to keep the lost area in the middle. It is considered that the selected area would provide sufficient data in order to fill the missing area.

In fact, in the first trials, the whole image was tested using the Kriging and RBF functions at once for both the Mask 5 and the 4 other masks. However, the functions needed during the operation of the array and the required meshgrid structures that need to be produced. When the results obtained for Mask 5 are evaluated; it is observed that Kriging and RBF methods produce better outputs. On the other hand, this advantage will be determined in the evaluation made through observation. The results obtained in Mask 5 can be compared visually with the study of Karaca and Tunga (2016). It is observed that the results obtained for staining of the quadratic region are much larger than the MSE values.

Corrupt Image	2D Cubic Interpolation	Kriging Interpolation	RBF Interpolation	HDMR Interpolation
noisy image 	PSNR, SSIM, MSE 35.4708 0.98133 18.4501 	PSNR, SSIM, MSE 35.3839 0.98003 18.8231 	PSNR, SSIM, MSE 35.8737 0.98199 16.8157 	PSNR, SSIM, MSE 35.4708 0.98133 18.4501 
noisy image 	PSNR, SSIM, MSE 36.6386 0.98506 14.1002 	PSNR, SSIM, MSE 36.6824 0.98489 13.9586 	PSNR, SSIM, MSE 37.0019 0.98596 12.9686 	PSNR, SSIM, MSE 36.6386 0.98506 14.1002 
noisy image 	PSNR, SSIM, MSE 31.2984 0.94543 48.221 	PSNR, SSIM, MSE 31.5 0.94765 46.0346 	PSNR, SSIM, MSE 31.537 0.94927 45.6438 	PSNR, SSIM, MSE 31.2984 0.94543 48.221 
noisy image 	PSNR, SSIM, MSE 31.4843 0.95225 46.2008 	PSNR, SSIM, MSE 31.1682 0.94965 49.6887 	PSNR, SSIM, MSE 31.4559 0.95172 46.5044 	PSNR, SSIM, MSE 31.4843 0.95225 46.2008 
noisy image 	PSNR, SSIM, MSE 35.4137 0.98282 18.6943 	PSNR, SSIM, MSE 35.8538 0.98423 16.8927 	PSNR, SSIM, MSE 36.8819 0.98407 13.3318 	PSNR, SSIM, MSE 35.4137 0.98282 18.6943 
noisy image 	PSNR, SSIM, MSE 36.7836 0.9828 13.637 	PSNR, SSIM, MSE 37.8719 0.98547 10.6143 	PSNR, SSIM, MSE 37.7299 0.98582 10.967 	PSNR, SSIM, MSE 36.7836 0.9828 13.637 
noisy image 	PSNR, SSIM, MSE 32.1876 0.94708 39.2938 	PSNR, SSIM, MSE 32.3014 0.9495 38.2768 	PSNR, SSIM, MSE 32.213 0.95041 39.0643 	PSNR, SSIM, MSE 32.1876 0.94708 39.2938 
noisy image 	PSNR, SSIM, MSE 29.2525 0.90391 77.2376 	PSNR, SSIM, MSE 29.1843 0.90206 78.4611 	PSNR, SSIM, MSE 29.2039 0.90416 78.1066 	PSNR, SSIM, MSE 29.2525 0.90391 77.2376 
noisy image 	PSNR, SSIM, MSE 26.7749 0.84485 136.6437 	PSNR, SSIM, MSE 26.096 0.82037 159.7656 	PSNR, SSIM, MSE 26.3119 0.82656 152.0166 	PSNR, SSIM, MSE 26.7749 0.84485 136.6437 

Figure 1 Grayscale sample image with in-painting

Corrupt Image	2D Cubic Interpolation	Kriging Interpolation	RBF Interpolation	HDMR Interpolation
<p>noisy image</p>	<p>PSNR, SSIM, MSE 37.3694 0.99657 11.9163</p>	<p>PSNR, SSIM, MSE 36.3132 0.99598 15.1973</p>	<p>PSNR, SSIM, MSE 36.1825 0.99586 15.6616</p>	<p>PSNR, SSIM, MSE 37.3481 0.99656 11.9747</p>
<p>noisy image</p>	<p>PSNR, SSIM, MSE 39.0467 0.99774 8.0986</p>	<p>PSNR, SSIM, MSE 37.8582 0.99718 10.6477</p>	<p>PSNR, SSIM, MSE 37.5792 0.99682 11.3542</p>	<p>PSNR, SSIM, MSE 39.0101 0.99773 8.1672</p>
<p>noisy image</p>	<p>PSNR, SSIM, MSE 33.0549 0.99038 32.1803</p>	<p>PSNR, SSIM, MSE 32.5236 0.98954 36.3678</p>	<p>PSNR, SSIM, MSE 32.4008 0.9892 37.4114</p>	<p>PSNR, SSIM, MSE 33.0204 0.99032 32.4369</p>
<p>noisy image</p>	<p>PSNR, SSIM, MSE 32.8171 0.99044 33.9917</p>	<p>PSNR, SSIM, MSE 31.3067 0.98766 48.1294</p>	<p>PSNR, SSIM, MSE 31.2143 0.98711 49.1643</p>	<p>PSNR, SSIM, MSE 32.8124 0.99044 34.0284</p>
<p>noisy image</p>	<p>PSNR, SSIM, MSE 36.1827 0.99591 15.6608</p>	<p>PSNR, SSIM, MSE 36.3019 0.99621 15.2367</p>	<p>PSNR, SSIM, MSE 36.7859 0.99637 13.63</p>	<p>PSNR, SSIM, MSE 36.1634 0.9959 15.7303</p>
<p>noisy image</p>	<p>PSNR, SSIM, MSE 39.9505 0.99786 6.577</p>	<p>PSNR, SSIM, MSE 41.0628 0.99835 5.091</p>	<p>PSNR, SSIM, MSE 40.443 0.99812 5.8719</p>	<p>PSNR, SSIM, MSE 39.9123 0.99785 6.6352</p>
<p>noisy image</p>	<p>PSNR, SSIM, MSE 34.9742 0.99332 20.685</p>	<p>PSNR, SSIM, MSE 34.9698 0.99342 20.7063</p>	<p>PSNR, SSIM, MSE 34.5287 0.99277 22.9197</p>	<p>PSNR, SSIM, MSE 34.9544 0.9933 20.7796</p>
<p>noisy image</p>	<p>PSNR, SSIM, MSE 31.5936 0.98569 45.0523</p>	<p>PSNR, SSIM, MSE 31.2815 0.98493 48.409</p>	<p>PSNR, SSIM, MSE 31.1229 0.98414 50.2096</p>	<p>PSNR, SSIM, MSE 31.5827 0.98567 45.1662</p>
<p>noisy image</p>	<p>PSNR, SSIM, MSE 28.6613 0.97254 88.501</p>	<p>PSNR, SSIM, MSE 27.9298 0.96815 104.7379</p>	<p>PSNR, SSIM, MSE 28.0026 0.96827 102.9969</p>	<p>PSNR, SSIM, MSE 28.659 0.97252 88.5482</p>

Figure 2 Colour sample image with in-painting

Table 2 Comparison of all images, masks and methods-Grayscale

		2D Cubic Interpolation			Kriging Interpolation			RBF Interpolation			HDMR Interpolation		
		PSNR	SSIM	MSE	PSNR	SSIM	MSE	PSNR	SSIM	MSE	PSNR	SSIM	MSE
Lena	Mask1	35.471	0.98133	18.45	35.384	0.98003	18.823	35.874	0.98199	16.816	35.471	0.98133	18.45
	Mask2	36.639	0.98506	14.1	36.682	0.98489	13.959	37.002	0.98596	12.969	36.639	0.98506	14.1
	Mask3	31.298	0.94543	48.221	31.5	0.94765	46.035	31.537	0.94927	45.644	31.298	0.94543	48.221
	Mask4	31.484	0.95225	46.201	31.168	0.94965	49.689	31.456	0.95172	46.504	31.484	0.95225	46.201
	Mask5	35.414	0.98282	18.694	35.854	0.98423	16.893	36.882	0.98407	13.332	35.414	0.98282	18.694
	Noise1	36.784	0.9828	13.637	37.872	0.98547	10.614	37.73	0.98582	10.967	36.784	0.9828	13.637
	Noise2	32.188	0.94708	39.294	32.301	0.9495	38.277	32.213	0.95041	39.064	32.188	0.94708	39.294
	Noise3	29.253	0.90391	77.238	29.184	0.90206	78.461	29.204	0.90416	78.107	29.253	0.90391	77.238
	Noise4	26.775	0.84485	136.64	26.096	0.82037	159.77	26.312	0.82656	152.02	26.775	0.84485	136.64
	Noise5	23.598	0.72678	283.94	23.019	0.69605	324.46	23.27	0.70052	306.23	23.598	0.72678	283.94
House	Mask1	40.928	0.98931	5.2512	40.359	0.9893	5.9872	39.515	0.9883	7.2715	40.928	0.98931	5.2512
	Mask2	43.898	0.99498	2.6504	43.479	0.99501	2.9186	42.548	0.99388	3.6162	43.898	0.99498	2.6504
	Mask3	37.635	0.97906	11.211	37.862	0.97944	10.64	36.753	0.97635	13.733	37.635	0.97906	11.211
	Mask4	35.842	0.97333	16.939	35.701	0.97317	17.497	34.682	0.96931	22.123	35.842	0.97333	16.939
	Mask5	38.951	0.98915	8.2782	40.742	0.99042	5.4816	43.857	0.99163	2.6756	38.951	0.98915	8.2782
	Noise1	47.819	0.99738	1.0744	47.855	0.99746	1.0657	45.775	0.99639	1.7201	47.819	0.99738	1.0744
	Noise2	37.905	0.9874	10.535	39.997	0.98683	6.5063	38.573	0.98345	9.0317	37.905	0.9874	10.535
	Noise3	36.898	0.97258	13.282	35.187	0.96611	19.697	34.445	0.96072	23.367	36.898	0.97258	13.282
	Noise4	32.53	0.934	36.314	30.709	0.91736	55.226	30.35	0.90886	59.994	32.53	0.934	36.314
	Noise5	25.212	0.82057	195.84	25.312	0.80812	191.38	25.289	0.80354	192.41	25.212	0.82057	195.84
Peppers	Mask1	39.189	0.99088	7.8374	39.631	0.99074	7.0791	39.416	0.99066	7.4377	39.189	0.99088	7.8374
	Mask2	42.063	0.99409	4.0435	42.656	0.99451	3.5274	41.299	0.99345	4.8212	42.063	0.99409	4.0435
	Mask3	35.572	0.97824	18.025	35.484	0.97721	18.396	35.288	0.97772	19.243	35.572	0.97824	18.025
	Mask4	32.549	0.96837	36.159	32.458	0.96667	36.926	31.916	0.96426	41.832	32.549	0.96837	36.159
	Mask5	32.701	0.98492	34.916	36.59	0.99072	14.257	36.018	0.99031	16.264	32.701	0.98492	34.916
	Noise1	42.558	0.99442	3.6084	42.964	0.99472	3.286	41.813	0.99402	4.2836	42.558	0.99442	3.6084
	Noise2	36.44	0.9797	14.758	36.079	0.97823	16.037	35.309	0.97622	19.151	36.44	0.9797	14.758
	Noise3	32.927	0.96034	33.146	32.572	0.9524	35.961	32.196	0.95017	39.22	32.927	0.96034	33.146
	Noise4	28.73	0.91716	87.117	27.579	0.88713	113.55	27.886	0.88925	105.8	28.73	0.91716	87.117
	Noise5	24.524	0.80588	229.46	24.03	0.77226	257.07	24.092	0.77667	253.46	24.524	0.80588	229.46
Mandrill	Mask1	33.607	0.9697	28.341	34.403	0.97272	23.591	34.308	0.97213	24.112	33.607	0.9697	28.341
	Mask2	35.45	0.98171	18.537	35.744	0.98254	17.325	35.505	0.98199	18.307	35.45	0.98171	18.537
	Mask3	29.277	0.92569	76.803	29.582	0.92778	71.59	29.385	0.92522	74.918	29.277	0.92569	76.803
	Mask4	29.17	0.92005	78.714	29.423	0.92242	74.256	29.178	0.91994	78.572	29.17	0.92005	78.714
	Mask5	37.325	0.98466	12.037	38.406	0.98865	9.3865	38.836	0.98899	8.5017	37.325	0.98466	12.037
	Noise1	35.096	0.98013	20.113	35.138	0.98042	19.921	34.633	0.97827	22.374	35.096	0.98013	20.113
	Noise2	29.509	0.92561	72.805	29.348	0.92245	75.555	29.118	0.91904	79.67	29.509	0.92561	72.805
	Noise3	26.259	0.84231	153.87	26.297	0.83673	152.53	26.035	0.83151	162.03	26.259	0.84231	153.87
	Noise4	23.592	0.71527	284.39	23.715	0.69501	276.4	23.381	0.69276	298.56	23.592	0.71527	284.39
	Noise5	21.045	0.48207	511.14	21.325	0.46271	479.25	21.189	0.473	494.53	21.045	0.48207	511.14
Jeplane	Mask1	35.763	0.98851	17.249	35.734	0.98738	17.363	35.419	0.98768	18.673	35.763	0.98851	17.249
	Mask2	36.561	0.99187	14.355	36.541	0.99196	14.422	35.943	0.9909	16.548	36.561	0.99187	14.355
	Mask3	31.514	0.96883	45.881	31.836	0.9692	42.605	31.48	0.96812	46.244	31.514	0.96883	45.881
	Mask4	30.23	0.96264	61.668	30.528	0.96125	57.586	30.098	0.96007	63.578	30.23	0.96264	61.668
	Mask5	34.77	0.99074	21.682	35.562	0.99056	18.067	35.175	0.99184	19.752	34.77	0.99074	21.682
	Noise1	39.482	0.99356	7.3265	39.906	0.99405	6.6453	38.988	0.99309	8.208	39.482	0.99356	7.3265
	Noise2	33.332	0.97603	30.188	33.393	0.97464	29.771	32.737	0.97209	34.625	33.332	0.97603	30.188
	Noise3	29.752	0.94846	68.848	29.742	0.94317	69.002	29.321	0.93934	76.032	29.752	0.94846	68.848
	Noise4	26.865	0.89929	133.82	25.929	0.87449	166.03	25.854	0.87406	168.91	26.865	0.89929	133.82
	Noise5	22.372	0.7664	376.59	22.087	0.73366	402.12	22.301	0.74699	382.77	22.372	0.7664	376.59

Table 3 Comparison of all images, masks and methods-Colour

		2D Cubic Interpolation			Kriging Interpolation			RBF Interpolation			HDMR Interpolation		
		PSNR	SSIM	MSE	PSNR	SSIM	MSE	PSNR	SSIM	MSE	PSNR	SSIM	MSE
Lena	Mask1	37.3690	0.9965	11.9160	36.3130	0.9959	15.1970	36.1820	0.9958	15.6620	37.3480	0.9965	11.9750
	Mask2	39.0470	0.9977	8.0986	37.8580	0.9971	10.6480	37.5790	0.9968	11.3540	39.0100	0.9977	8.1672
	Mask3	33.0550	0.9903	32.1800	32.5240	0.9895	36.3680	32.4010	0.9892	37.4110	33.0200	0.9903	32.4370
	Mask4	32.8170	0.9904	33.9920	31.3070	0.9876	48.1290	31.2140	0.9871	49.1640	32.8120	0.9904	34.0280
	Mask5	36.1827	0.9959	15.6608	36.3019	0.9962	15.2367	36.7859	0.9963	13.6300	36.1634	0.9959	15.7303
	Noise1	39.9510	0.9978	6.5770	41.0630	0.9983	5.0910	40.4430	0.9981	5.8719	39.9120	0.9978	6.6352
	Noise2	34.9740	0.9933	20.6850	34.9700	0.9934	20.7060	34.5290	0.9927	22.9200	34.9540	0.9933	20.7800
	Noise3	31.5940	0.9856	45.0520	31.2820	0.9849	48.4090	31.1230	0.9841	50.2100	31.5830	0.9856	45.1660
	Noise4	28.6610	0.9725	88.5010	27.9300	0.9681	104.7400	28.0030	0.9682	103.0000	28.6590	0.9725	88.5480
	Noise5	24.5101	0.9364	230.1814	24.1843	0.9302	248.1129	24.2096	0.9303	246.6749	24.4822	0.9359	231.6658
House	Mask1	40.4790	0.9959	5.8238	39.4160	0.9947	7.4390	39.0240	0.9945	8.1407	40.4790	0.9959	5.8238
	Mask2	41.5140	0.9972	4.5883	41.4500	0.9970	4.6565	41.0230	0.9968	5.1379	41.5140	0.9972	4.5885
	Mask3	35.6460	0.9892	17.7200	34.4480	0.9863	23.3500	34.0940	0.9858	25.3320	35.6460	0.9892	17.7200
	Mask4	33.9880	0.9850	25.9600	32.7490	0.9813	34.5320	32.3050	0.9801	38.2500	33.9880	0.9850	25.9590
	Mask5	40.0240	0.9977	6.4662	39.3290	0.9968	7.5886	41.6210	0.9986	4.4765	40.0240	0.9977	6.4662
	Noise1	42.5520	0.9973	3.6128	41.9370	0.9972	4.1625	41.3550	0.9968	4.7599	42.7410	0.9973	3.4590
	Noise2	35.5040	0.9889	18.3090	35.6730	0.9890	17.6100	35.3360	0.9880	19.0300	35.7270	0.9891	17.3920
	Noise3	32.6610	0.9779	35.2370	32.2310	0.9763	38.9060	32.0950	0.9752	40.1400	33.0250	0.9783	32.4040
	Noise4	29.3080	0.9565	76.2580	28.4140	0.9476	93.6950	28.5930	0.9482	89.9060	29.9980	0.9572	72.9990
	Noise5	24.8730	0.8977	211.7300	24.5450	0.8880	228.3600	24.5710	0.8889	226.9800	25.0030	0.8994	205.5100
Peppers	Mask1	36.7600	0.9964	13.7130	34.0110	0.9944	25.8200	35.1310	0.9955	19.9530	34.7740	0.9932	21.6610
	Mask2	39.0040	0.9973	8.1792	38.1130	0.9970	10.0420	38.1140	0.9972	10.0400	36.1120	0.9942	15.9170
	Mask3	32.7020	0.9898	34.9060	32.0700	0.9888	40.3730	32.0650	0.9892	40.4210	31.5940	0.9860	45.0530
	Mask4	30.5920	0.9852	56.7340	28.9100	0.9800	83.5830	29.1750	0.9812	78.6360	29.7810	0.9812	68.3920
	Mask5	32.510	0.9962	36.4840	35.3340	0.9976	19.0400	35.4160	0.9977	18.6830	31.7720	0.9934	43.2440
	Noise1	37.0490	0.9960	12.8290	37.3210	0.9963	12.0500	37.3460	0.9964	11.9800	35.0560	0.9929	20.3010
	Noise2	31.9010	0.9873	41.9780	31.9410	0.9876	41.5890	32.0020	0.9878	41.0100	30.7700	0.9830	54.4590
	Noise3	29.2230	0.9769	77.7570	28.9520	0.9758	82.7650	29.0920	0.9765	80.1390	28.4840	0.9716	92.1980
	Noise4	26.9580	0.9621	131.0100	26.0360	0.9550	161.9900	26.2500	0.9565	154.1800	26.0540	0.9523	161.3300
	Noise5	23.1160	0.9209	317.3300	22.8300	0.9129	338.9300	22.8610	0.9130	336.5100	22.2150	0.8988	390.4300
Mandrill	Mask1	32.5990	0.9813	35.7410	32.1320	0.9806	39.8000	31.7410	0.9793	43.5520	32.5970	0.9813	35.7550
	Mask2	34.1960	0.9884	24.7460	34.2940	0.9887	24.1930	34.0950	0.9882	25.3270	34.1920	0.9884	24.7660
	Mask3	28.5570	0.9525	90.6530	28.4160	0.9498	93.6420	28.2680	0.9487	96.8830	28.5600	0.9525	90.5800
	Mask4	28.4080	0.9535	93.8250	28.0750	0.9526	101.3000	27.5810	0.9496	113.4800	28.4070	0.9535	93.8400
	Mask5	31.6180	0.9898	44.8000	30.8770	0.9922	53.1310	32.6760	0.9933	35.1160	31.6170	0.9898	44.8140
	Noise1	33.9730	0.9854	26.0490	34.0290	0.9852	25.7150	33.7550	0.9844	27.3870	33.9720	0.9854	26.0570
	Noise2	28.6800	0.9484	88.1250	28.7050	0.9475	87.6170	28.5010	0.9456	91.8380	28.6800	0.9484	88.1200
	Noise3	25.6260	0.8935	178.0400	25.6400	0.8903	177.4400	25.5230	0.8893	182.2900	25.6230	0.89354	178.1300
	Noise4	23.1580	0.8132	314.2800	23.0380	0.80268	323.0300	22.9140	0.8021	332.4000	23.1540	0.81314	314.5200
	Noise5	20.4720	0.6666	583.3300	20.6280	0.66629	562.7500	20.5690	0.6665	570.4300	20.4700	0.66662	583.5400
Jeplane	Mask1	37.1680	0.9923	12.4810	36.6330	0.9904	14.1190	35.7000	0.9897	17.5000	37.1600	0.99237	12.5040
	Mask2	38.4190	0.9942	9.3570	37.6990	0.99307	11.0440	37.4830	0.9928	11.6100	38.4120	0.99428	9.3736
	Mask3	32.2060	0.9772	39.1250	31.6920	0.97279	44.0430	31.4280	0.9729	46.8000	32.1880	0.97726	39.2910
	Mask4	30.5990	0.9713	56.6480	29.3490	0.96121	75.5430	29.1340	0.9606	79.3740	30.5970	0.97132	56.6740
	Mask5	35.4370	0.9909	18.5940	36.6620	0.99098	14.0250	36.6260	0.9922	14.1420	35.4320	0.99091	18.6170
	Noise1	39.8120	0.9950	6.7904	39.7660	0.99492	6.8626	38.9670	0.9943	8.2479	39.7950	0.99509	6.8170
	Noise2	33.7350	0.9817	27.5160	33.5000	0.97901	29.0470	33.0860	0.9781	31.9500	33.7190	0.98176	27.6190
	Noise3	30.4710	0.9604	58.3400	29.6470	0.94927	70.5260	29.5550	0.9501	72.0480	30.4650	0.96044	58.4200
	Noise4	27.0080	0.9208	129.5100	25.9770	0.8900	164.2200	25.8960	0.8922	167.2800	26.9900	0.9207	130.0300
	Noise5	22.3250	0.8036	380.7200	22.4040	0.76772	373.8400	22.4520	0.7792	369.7000	22.3390	0.80356	379.4600

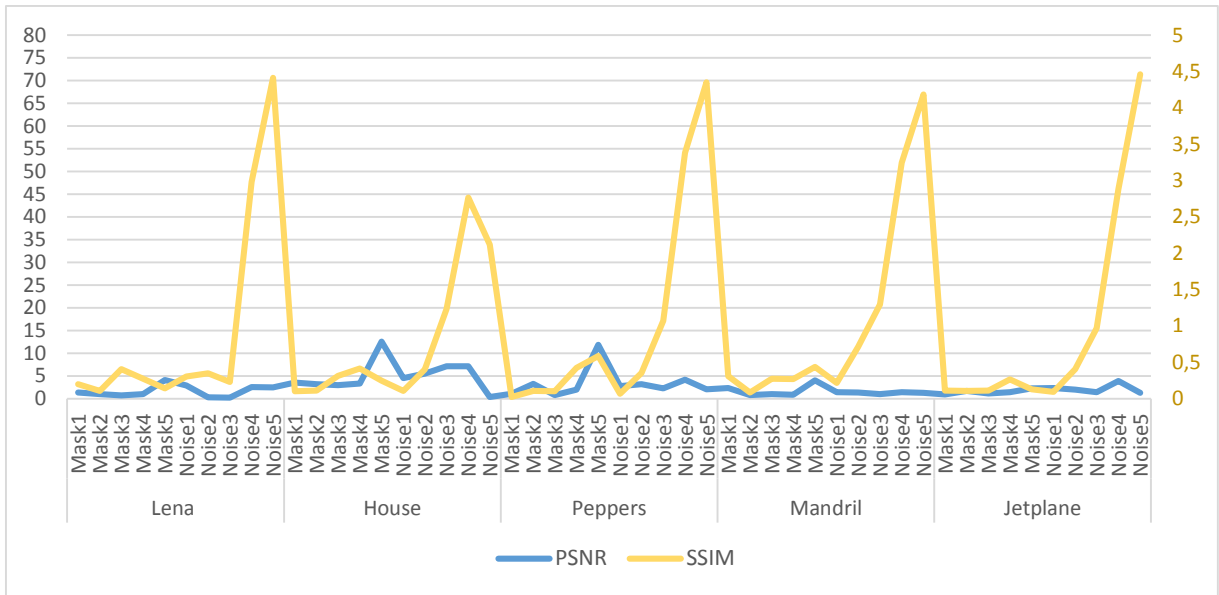


Figure 3 Percentage variation of the difference between the highest and lowest values of PSNR, SSIM scores obtained from grayscale images

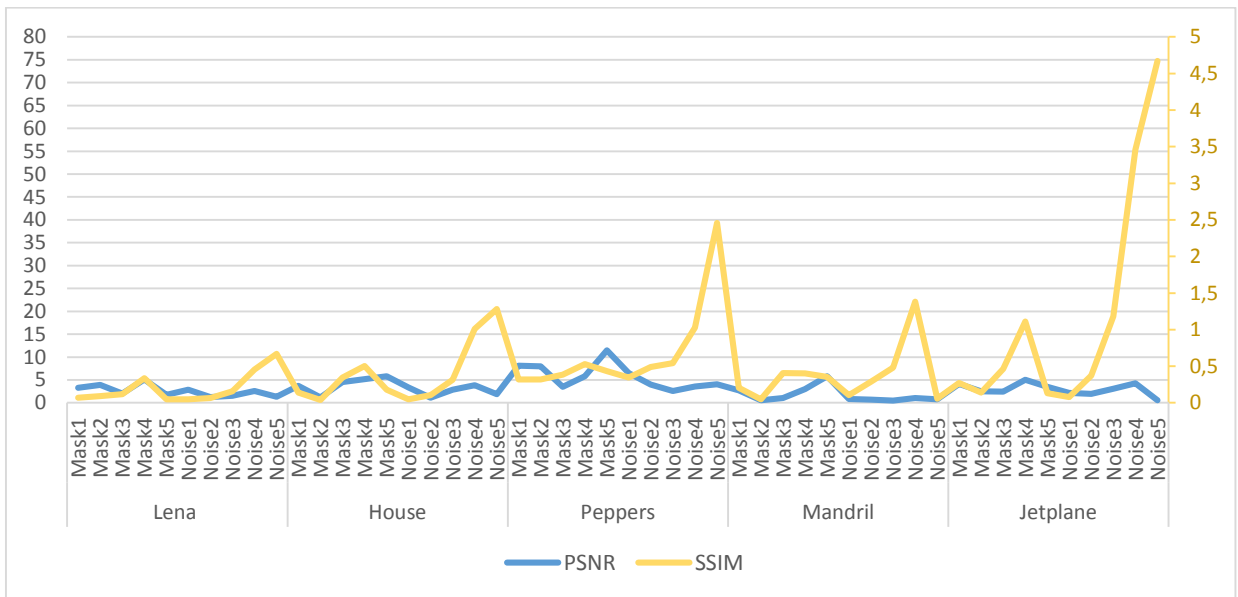


Figure 4 Percentage variation of the difference between the highest and lowest values of PSNR, SSIM scores obtained from colour images

According to the results, the square area is still clearly visible and filled with diagonal lines. In our results, the square area (for Kriging and RBF interpolation) was less prominent and no diagonal lines were observed in the faulty area. The difference between grayscale and colour images of the two studies may be inaccurate, but the interiors of in-painting characters can still be observed. Although relatively, the results obtained in our study can be more visually appealing.

5. Conclusion

The literature lacks a detailed evaluation on the use of interpolation methods for the in-painting problem. Accordingly, this study aimed to evaluate state-of-the-art approaches, namely, two dimensional cubic, Kriging, RBF and YBMG based Lagrange interpolation methods, which are recently studied in the literature.

A benchmark dataset was generated in order to perform a detailed evaluation of the in-painting algorithms. Several comprehensive experiments were conducted in order to make a fair assessment. According to the results obtained, it is observed that the methods do not have absolute superiority to each other in terms of in-painting results. However, Kriging and RBF interpolation produce better results both for numerical data and visual evaluation for image in-painting problems having large area losses. Studies on this subject have also yielded good results for large area in-painting, but Kriging and RBF interpolation outputs look better in terms of visual quality.

References

- Altın, E. M., & Tunga, B. (2014). High Dimensional Model Representation in Image Processing. *Proceedings of the 14th International Conference on Computational and Mathematical Methods in Science and Engineering, CMMSE*, 55–64. <https://doi.org/10.1063/1.4904687>
- Amasidha, K. S., Awati, A. S., Deshpande, S. P., & Patil, M. R. (2016). Digital Image Inpainting: A Review. *International Research Journal of Engineering and Technology (IRJET)*, 03(01), 851–854. Tarihinde adresinden erişildi <https://www.irjet.net/archives/V3/i1/IRJET-V3I1150.pdf>
- Awati, A. S., Deshpande, S. P., Belagal, P. Y., & Patil, M. R. (2017). Digital Image Inpainting Using Modified Kriging Algorithm. *2nd International Conference for Convergence in Technology (I2CT)*, 945–950.
- Bertalmio, M., Sapiro, G., Caselles, V., & Ballester, C. (2000). Image Inpainting. *SIGGRAPH Proceedings of the 27th annual conference on Computer graphics and interactive techniques*, 417–424.
- Bostanci, E., (2014). Is Hamming distance only way for matching binary image feature descriptors?, *Electronics Letter* 50(11), 806-808
- Bugeau, A., Bertalmío, M., Caselles, V., & Sapiro, G. (2010). A Comprehensive Framework for Image Inpainting. *IEEE Transactions on Image Processing*, 19(10), 2634–2645.
- Chang, L., & Chongxiu, Y. (2011). New Interpolation Algorithm for Image Inpainting. İçinde *International Conference on Physics Science and Technology (ICPST)* (C. 22, ss. 107–111). Elsevier B.V. <https://doi.org/10.1016/j.phpro.2011.11.017>
- Foster, M. (2009). MATLAB Multivariate Interpolation Toolbox. Tarihinde 01 Eylül 2018, adresinden erişildi <https://github.com/mattfoster/matlab-interpolation-toolkit>
- Guzel M.S. (2015) , Performance evaluation for feature extractors on street view images, *The Imaging Science Journal*, 64(1), 26-33.
- Horé, A., & Ziou, D. (2010). Image quality metrics : PSNR vs . SSIM. İçinde *International Conference on Pattern Recognition* (ss. 2366–2369). <https://doi.org/10.1109/ICPR.2010.579>
- Jassim, F. A. (2013). Image Inpainting by Kriging Interpolation Technique. *World of*

- Computer Science and Information Technology Journal (WCSIT)*, 3(5), 91–96.
- Jassim, F. A. (2013). Kriging Interpolation Filter to Reduce High Density Salt and Pepper Noise, 3(1), 8–14.
- Karaca, E., & Tunga, M. A. (2016a). A Method for Inpainting Rectangular Missing Regions using High Dimensional Model Representation and Lagrange Interpolation. *24th Signal Processing and Communication Application Conference (SIU) Signal Processing and Communication Application Conference (SIU)*.
- Karaca, E., & TUNGA, M. A. (2016b). Interpolation-Based Image Inpainting in Colour Images Using High Dimensional Model Representation. *24th European Signal Processing Conference (EUSIPCO)*, 2425–2429. <https://doi.org/10.1109/EUSIPCO.2016.7760684>
- Mutlu, B., Hacıomeroglu, M., Guzel, M.S. et al. (2014). Silhouette Extraction from Street View Images, *International Journal of Advanced Robotic Systems*, 1-12 .
- Sapkal, M. S., & Kadbe, P. (2016). Kriging Interpolation Technique Basis Image Inpainting. *International Journal of Latest Trends in Engineering and Technology (IJLTET)*, 6(3), 467–470.
- Sapkal, M. S., Kadbe, P. K., & Deokate, B. H. (2016). Image Inpainting By Kriging Interpolation Technique For Mask Removal. *International Conference on Electrical, Electronics, and Optimization Techniques (ICEEOT)*, 310–313.
- Seref , B., Bostanci, G. E, Guzel, M.S. (2021). Evolutionary neural networks for improving the prediction performance of recommender systems, *Turkish Journal of Electrical Engineering & Computer Sciences*, 29(1), 62-77.
- Schwanghart, W., & Kuhn, N. J. (2010). TopoToolbox : A set of Matlab functions for topographic analysis. *Environmental Modelling and Software*, 25, 770–781. <https://doi.org/10.1016/j.envsoft.2009.12.002>
- Tunga, B., & Koçanaoğulları, A. (2017). Digital image decomposition and contrast enhancement using high-dimensional model representation. *Signal, Image and Video Processing*, 299–306. <https://doi.org/10.1007/s11760-017-1158-8>
- Wang, W., & Qin, X. (2006). An Image Inpainting Algorithm Based on CSRBF Interpolation. *Dianzi Yu Xinxu Xuebao/Journal of Electronics and Information Technology*, 890–894.